

Interfacial deformation and failure mechanisms at the single-splat length scale revealed in-situ by indentation of cold sprayed aluminum microparticles



Pranjal Nautiyal ^{a,1}, Cheng Zhang ^a, Benjamin Boesl ^a, Arvind Agarwal ^{a,*}

^a Department of Mechanical and Materials Engineering, Florida International University, 10555 West Flagler Street, Miami, FL, 33174, USA

ARTICLE INFO

Keywords:
Cold spray
Splats
In-situ indentation
Interface bonding
Deformation mechanisms

ABSTRACT

Cold spray deposition exploits the phenomenon of impact bonding for solid-state consolidation of metallic microparticles. However, the particle interfaces in the deposits are susceptible to crack propagation under mechanical stresses, which results in inferior ductility. In this work, we seek to develop insights into splat-substrate interface bonding by in-situ micromechanical investigations. A miniaturized mechanical testing approach is reported here, which relies on micromachining, targeted indentation, and real-time scanning electron microscopy to probe deformation and failure at buried interfaces. Investigations at the “single splat length scale” enabled us to distinguish deformation mechanisms associated with 6061Al splats with globular and pancake-shaped morphologies. We observed a transition from mechanical interlocking to metallurgical bonding with an increase in the degree of particle flattening during deposition. The mechanically interlocked splats debond from the substrate via crack propagation and splat sliding. On the other hand, metallurgically bonded splats do not fail under indentation stresses exceeding 380 MPa; instead, displaying shear band propagation and pile-up mechanisms. A four-fold enhancement in the critical stress for crack propagation in mechanically-interlocked splats is achieved after a two-step annealing-aging heat-treatment cycle. We demonstrate that interface bonding plays a more dominant role than the inherent plasticity of splats in influencing bulk deposits’ ductility, underscoring the importance of interface engineering in cold sprayed materials.

1. Introduction

The phenomenon of impact-bonding has gained renewed scrutiny due to growing interest in metal additive manufacturing [1–5]. Cold spray, a solid-state consolidation process, involves accelerating micron-sized powder particles to supersonic velocities followed by severe plastic deformation as they encounter a substrate [6]. The plastic strains at the interacting surface of microparticles during impact can exceed 1000 % [7], leading to significant flattening and forming pancake-shaped structures called splats [8]. Mechanical interlocking and metallurgical bonding are believed to be the two key bonding mechanisms at splat-substrate and splat-splat interfaces [9]. The nature of bonding depends on the impact velocity [10–12], the density, and the hardness of microparticles with respect to the substrate [13,14], oxide coating on microparticles [15,16], and the roughness of the substrate

[9]. Metallurgical bonding is stronger and desirable, owing to the atomic level contact and chemical interactions between the elements [17,18]. High particle impact velocities ($>v_{critical}$) lead to jetting and surface oxide removal [19], enabling clean metal-to-metal contact for chemical bonding [20]. Therefore, meeting the velocity threshold for jetting is a crucial consideration while selecting cold spray parameters [21]. However, jetting is localized to the interacting particle surface periphery, leading to non-homogeneous bonding [22]. Moreover, ultrashort timescales and modest temperatures (compared to other thermal spray techniques [23]) limit the extent of interface diffusion possible. The resulting micro-cracks at splat-substrate and splat-splat interfaces can have deleterious effects on cold sprayed deposits’ mechanical properties. Sundararajan and co-workers reported a loss in elastic modulus of a wide range of cold-sprayed metals, such as Cu, Zn, Ti, Ta, Nb, and stainless steel compared to their bulk counterparts [24]. A strong

* Corresponding author. Department of Mechanical and Materials Engineering, Florida International University, 10555 West Flagler Street, Miami, FL, 33174, USA.
E-mail address: agarwala@fiu.edu (A. Agarwal).

¹ Author’s current address: Department of Mechanical Engineering and Applied Mechanics, University of Pennsylvania, 220 S. 33rd St., Philadelphia, PA, 19104, USA

negative correlation between coating modulus and inter-splat crack density was noticed, with a considerable ~40 % modulus loss even at a low inter-splat crack density of less than 10 %. Cold sprayed deposits are characterized by high flow stresses due to work hardening during deposition [25], but they display arrested ductility. Rokni et al. reported ~3 % strain to fracture during a micro tensile investigation of 6061Al deposits, which is merely one-third the failure strain of a 6061Al-T6 alloy [26]. Weakly-bonded interfaces become preferred sites for crack nucleation and propagation under external mechanical loading [27,28], responsible for arrested plasticity and premature failure in cold-sprayed deposits. This is particularly problematic for applications where fatigue resilience is important. Gavras and co-workers reported the threshold for crack propagation (ΔK_{th}) in as-sprayed 6061Al coating was merely 60 % of the threshold for the rolled alloy [29]. Post-spray heat-treatment has been reported to be advantageous to eliminate micro-cracks and promote bonding [24,30], augmenting mechanical properties of deposits [31–33]. However, inter-particle cracking, although arrested after heat-treatment, remains a cause of concern [26,34].

Our prior study on in-situ strain evolution in the cold sprayed 6061Al subjected to four-point bending revealed the coatings do not deform as a single rigid body [35]. Instead, individual splats experience different degrees of plastic strain, activating the splat sliding mechanism [36,37]. The non-homogeneous strain distribution was particularly pronounced for coatings with higher inter-splat porosity, suggesting splat sliding is a product of inferior interface bonding. We presented visual evidence of these tensions in the microstructure by conducting in-situ indentation creep tests inside the scanning electron microscope (SEM) as a function of temperature [38]. It was observed that thermo-mechanical stresses during indentation are concentrated along the splat boundaries, leading to crack initiation, propagation, and splat delamination. Therefore, it is pertinent to examine the adhesion, deformation, and failure characteristics at interfaces to overcome the challenges described above with cold sprayed deposits' mechanical properties. The bulk of work in the literature on interface-related mechanical phenomena relies on post-failure imaging of deposits [26,27,39]. There are some limitations associated with this approach. First, it's challenging to isolate interfacial phenomena, such as inter-splat cracking, from intrinsic characteristics like the plastic deformation of particles. Secondly, the mechanistic understanding is primarily qualitative, and there is a lack of information on the critical stresses required to activate different deformation and failure mechanisms. Given the fact that splats are the building blocks of cold sprayed deposits, interface bonding is an essential consideration to develop high-performance deposits. The adhesion of coatings on substrates is routinely characterized by various tests, such as tensile pull-off, three-lug shear, and collar-pin pull-off test [26,40]. While these tests are essential to developing coatings with high adherence to the substrate, they do not provide a precise understanding of bonding mechanisms at the single splat length scale. This information deficit limits our current understanding of how different bonding modes contribute to cold sprayed deposits' mechanical properties.

A significant impediment to single splat testing is the miniature sample size (μm -sized particles), difficult to resolve for targeted mechanical loading. Another challenge is that the splat-substrate interfaces are buried and hidden from view, preventing direct observation of deformation and failure phenomena. In this work, we report a miniature mechanical testing approach based on in-situ indentation of micro-machined splats inside the SEM, permitting real-time imaging of deformation mechanisms activated at the interface. This method harnesses the multi-axial stress field beneath the indenter probe [41] to trigger interface deformation and failure. We examined the effect of varying plastic strain (extent of particle deformation/flattening) during supersonic impact and post-spray heat-treatment on the nature of bonding at splat-substrate interfaces. The findings in this work will pave the way for devising interface engineering strategies to develop cold sprayed deposits with superior mechanical properties.

2. Experimental section

2.1. Cold spray and post-deposition heat-treatment

Gas atomized 6061Al powder particles with an average size of 38.7 μm (Valimet, CA, USA) were used in this work. Splats with two distinct morphologies, globular (Fig. 1a) and pancake-shaped (Fig. 1b), were deposited on a clean, polished 6061Al (T6) substrate using a high-pressure CGT 4000 cold spray system (CGT Technologies, Munich, Germany). A custom-developed steel screen with tiny holes (~1 mm radius) was placed in front of the substrate to achieve discrete splat deposition. Two sets of processing conditions were used to obtain the morphologies mentioned above: (a) air as the carrier gas with a pressure and temperature of 6.2 MPa and 451 °C at the gun, respectively, and (b) Helium as the carrier gas with pressure and temperature of 3.45 MPa and 384.3 °C, respectively. The selection of these spray conditions is based on a prior article by the authors, where the role of processing gases on coating microstructure was examined [35]. The deposition was performed with a single pass to avoid coating build-up. Fig. S1 in the supporting information shows the successful deposition of splats.

The nature of bonding at the splat/substrate interface was tailored by

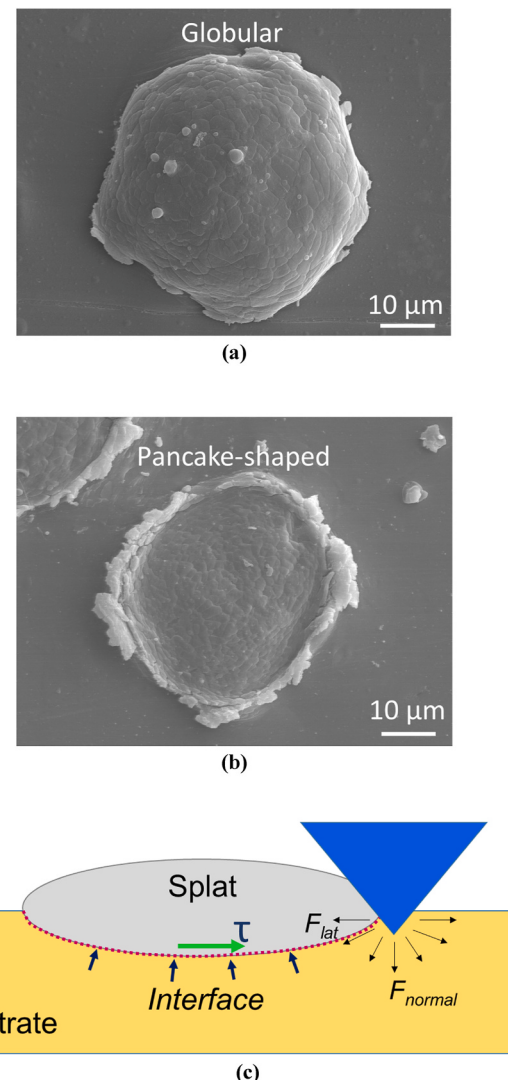


Fig. 1. SEM images showing splats with globular (a) and pancake-shaped (b) morphologies, and (c) schematic representation of indentation-based test method to probe interfacial deformation behavior at the single splat length scale.

a two-step heat-treatment cycle, consisting of solution treatment and aging treatment, using standard T6 conditions for 6061Al alloy [42]. The solution treatment was performed at 530 °C for 50 min (followed by water quenching), while aging was carried out at 160 °C for 18 h (followed by air cooling).

2.2. In-situ test method

The adhesion of plasma-sprayed splats has been reported by the nanoscratch technique, which harnesses force exerted by a moving indenter probe to de-bond and displace a splat from its original location [43,44]. However, scratch-based methods are challenging to implement for cold sprayed interfaces since metallic microparticles are embedded inside the substrate due to severe plastic deformation in the interaction zone. The interlocked interfaces resist de-bonding due to scratch-induced forces. We observed scratch-loading results in plastic deformation and/or wear of splats (shown in [Supplementary Video V1](#), [Fig. S2](#)). To overcome this challenge, we developed a novel test method based on targeted indentation of the substrate at the periphery of splats. Indentation loading results in a multi-axial stress-state beneath the tip [45]. Our approach harnesses the stress-field's horizontal component (F_{lat}) to induce localized interface debonding, schematically shown in [Fig. 1c](#). The in-situ indenter used for these investigations (Picoindenter, Hysitron PI 87, Bruker, USA) is equipped with a lateral load sensor to measure the horizontal forces, in addition to the normal forces typically captured during indentation. The tests were performed in displacement control mode, with the maximum penetration depth of the same order of magnitude as the size of splats (~10 µm) to trigger interface de-bonding. A 60 s hold step was programmed prior to indentation for thermal drift correction. A diamond conospherical probe with a 1 µm radius was used for these investigations. The testing was performed inside an SEM (JEOL JIB-4500, Tokyo, Japan), which allowed us to identify, resolve and test micron-sized splats. Real time imaging enabled the correlation of the lateral force readings with splat debonding/deformation mechanisms. An upward of 20 splat specimens were tested for each processing/post-processing condition. The splats were sectioned by focused ion beam (FIB) milling prior to in-situ indentation to be able to visualize the underlying mechanisms governing interfacial deformation and debonding.

3. Results

[Fig. 2a](#) demonstrates an in-situ indentation experiment performed on a globular splat. Targeted substrate loading near the splat periphery resulted in the splat's horizontal displacement away from the probe. The horizontal component of the multi-axial stress field beneath the tip pushes the splat in the negative x-direction. However, there is a resistance against splat displacement initially due to interface bonding between the splat and the substrate. The opposition against splat displacement is exerted in the form of interfacial shear stress in the positive x-direction (illustrated in [Fig. 1c](#)). There is a build-up of stress until a critical lateral force (F_{cr}), after which the interface succumbs to the externally applied load, and the splat is displaced from its original position. By capturing horizontal force readings using a lateral force sensor, we were able to quantify the load required to trigger splat sliding. [Fig. 2b](#) shows the lateral force variation as a function of normal displacement (tip penetration). There is a point of maxima in the force curve, which we refer to as the critical point for failure initiation. The splat displacement event is characterized by a drop in the lateral force value (negative slope), which can be ascribed to the release of stress built up at the interface up to the critical point. [Supplementary Video V2](#) demonstrates indentation-induced sliding of a globular splat. Interestingly, we did not observe the splat displacement phenomenon when the same experiment was repeated for the pancake-shaped splats ([Supplementary Video V3](#)). Instead, there was local plastic deformation around the point of tip penetration.

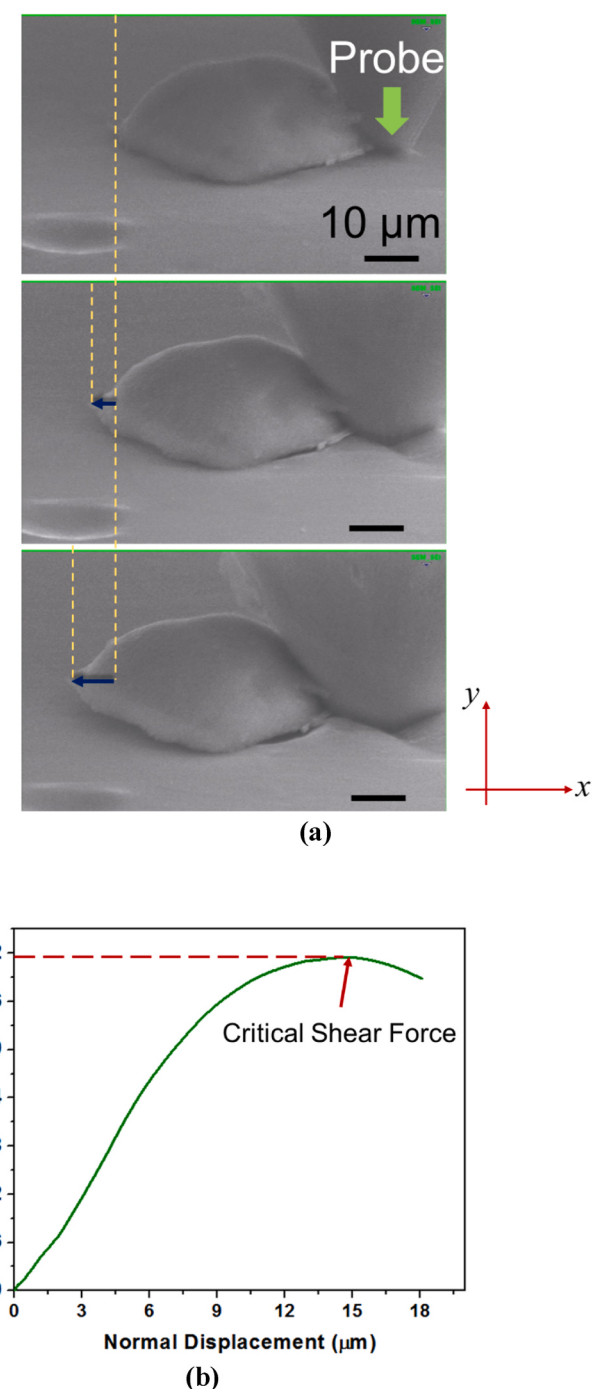


Fig. 2. (a) In-situ imaging of indentation-induced splat displacement, and (b) lateral force vs. normal displacement plot for identifying critical shear force for activating splat sliding in a globular splat.

From the experiment demonstrated in [Fig. 2](#), we can only observe the horizontal movement of the splat. It is unclear what transpires beneath the splat leading up to the displacement event. To unravel the mechanisms activated due to indentation loading, we sectioned the splats by focused ion beam machining ([Fig. 3a](#)), exposing the splat/substrate interface ([Fig. 3b, c](#)). There is a noticeable variation in the nature of bonding for air-sprayed globular splats. While some of the splats were characterized by intimate contact, others had incomplete bonding, micro-cracks, and even prominent porosity (shown in [Fig. 3b](#)). Contrary to this, He-sprayed pancake-shaped splats always displayed intimate bonding without any discernible gaps or micro-cracks ([Fig. 3c](#)). These

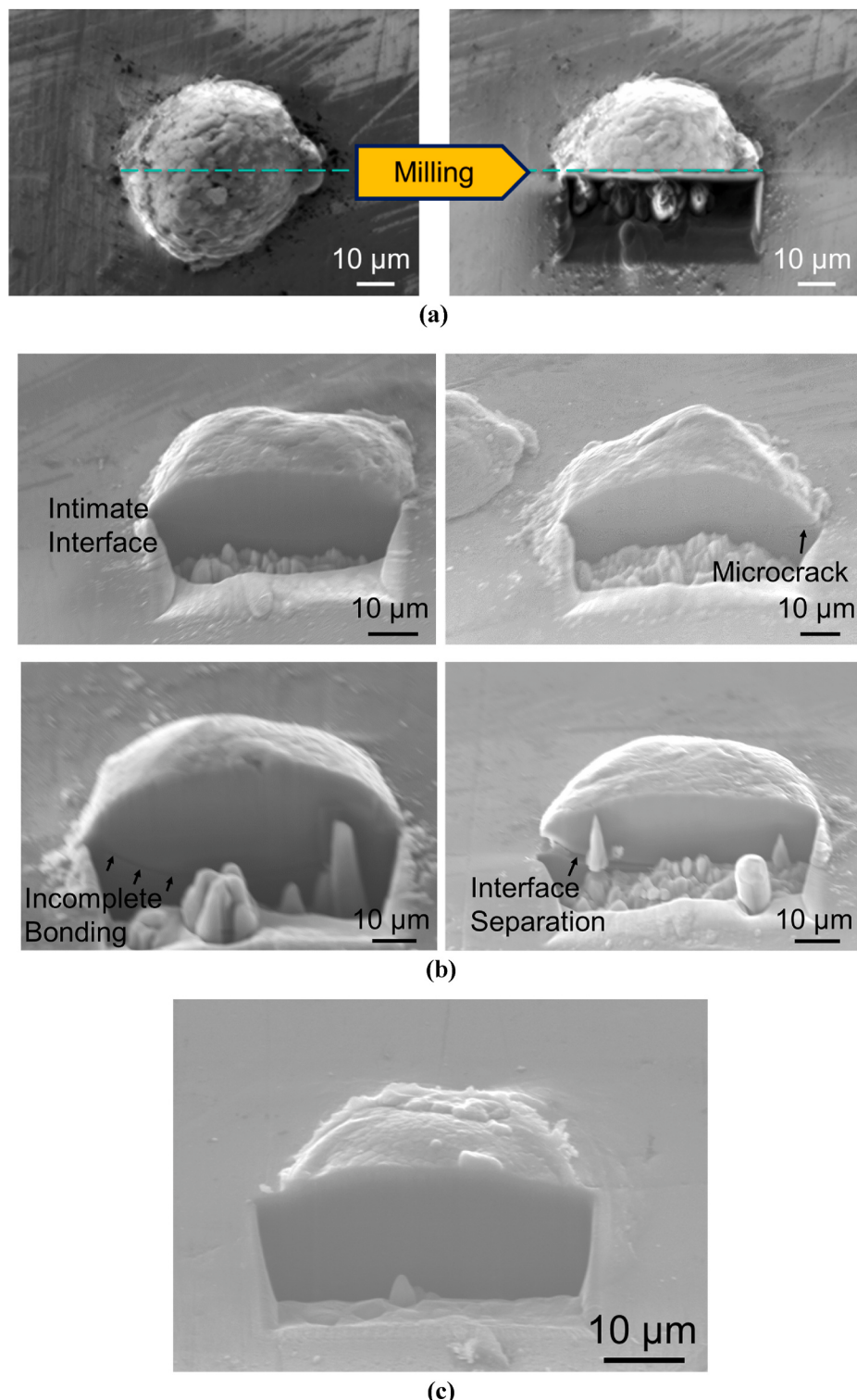


Fig. 3. (a) FIB milling to section the splats and SEM imaging of exposed splat-substrate interfaces revealing the nature of bonding in globular (b) and pancake-shaped (c) splats.

dissimilarities arise due to the difference in the sonic velocity (ν) in the two gases, governed by the relationship, $\nu = \sqrt{\gamma RT/A}$ [46], where γ is the specific heat ratio of the gas, A is the carrier gas's molecular weight, T is temperature, and R is the universal gas constant. Helium gas has a higher specific heat ratio and lower molecular weight, favorable for superior sonic velocity. Therefore, particles sprayed with He as the carrier gas are accelerated to higher velocities before impact, which

results in severe plastic deformation of microparticles and produces intimate splat-substrate bonding. On the other hand, particles sprayed using air as the carrier gas impact the substrate with lower velocity, and hence, the interface bonding is incomplete. The differences in interface bonding seen for air-sprayed splats (Fig. 3b) can be attributed to the variations in microparticle diameter (d), which has a negative correlation with the critical impact velocity, $V_{crod}d^{-n}$ [21], exponent n being 0.19 for Al [47]. Smaller-sized particles possess lower kinetic energy,

resulting in arrested adiabatic heating and interface softening, leading to relatively inferior bonding (compared to larger splats). Additionally, variations in individual microparticles' velocity are expected depending on their relative location in the spray stream. Minor differences in impact velocity may produce significant variations in interface bonding if the impact conditions are very close to the critical velocity.

We again performed indentation loading of the substrate near the machined splats' edge after exposing the interface. Fig. 4a demonstrates the buildup of stress at the interface during indentation loading, eventually leading to debonding and displacement of the splat from its original position. In some cases, splat displacement was preceded by crack initiation, advancement, and deflection events (Fig. 4b). The tortuous crack propagation is indicative of "interlocking" between the splat and the substrate. In the interlocking mechanism, there is physical interpenetration between the splat and the substrate. These interpenetrating networks disrupt a propagating crack, delaying splat debonding (Supplementary Videos V4). The critical stress required for activating splat sliding (σ_{ss}) can be estimated based on the critical shear

force value (shown in the force plot in Fig. 2b) and the area of contact between the splat and the substrate (A_{interf}):

$$\sigma_{ss} = \frac{F_{cr}}{A_{interf}} \quad (1)$$

Assuming the spherical microparticles transform to half-ellipsoids upon impact [11], the resulting splat/substrate contact area can be expressed as, $A_{interf} = \pi d^2/2$, d being the diameter of the original spherical particles. Calculations based on Eq. (1) revealed a bimodal distribution of σ_{ss} , shown in Fig. 4c. While splats with intimate interface were characterized by $\sigma_{ss} \sim 1600$ kPa, incompletely or poorly bonded splats were susceptible to splat sliding at stresses as low as 450 kPa.

It was shown in Supplementary Video V3 that the pancake-shaped splat could not be displaced during indentation loading. This was a consistent observation during the in-situ testing of multiple splats. To understand where the mechanical work done during tip penetration is expended, we sectioned these splats by FIB milling and repeated indentation testing to observe the interfacial mechanisms. In striking

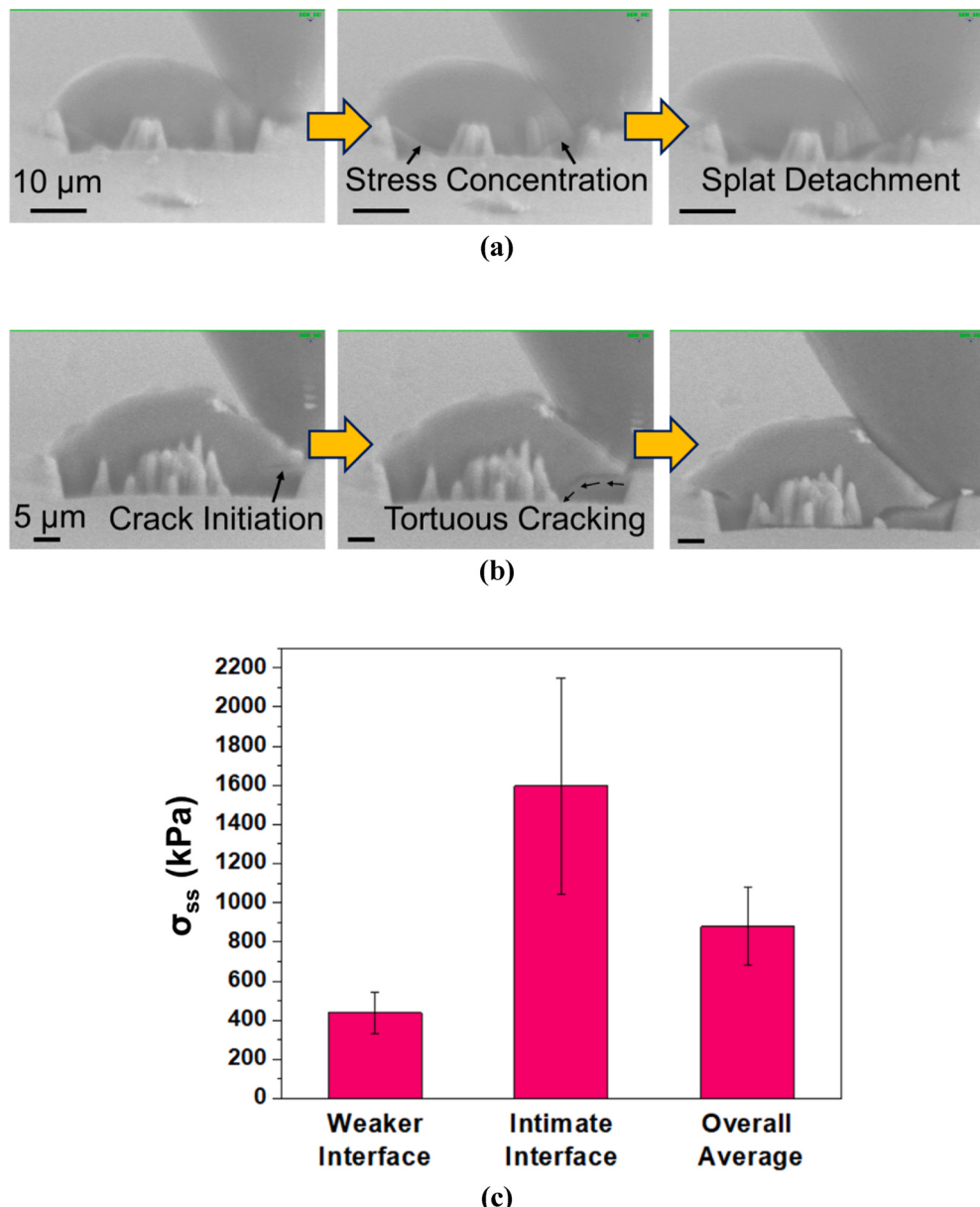


Fig. 4. Real-time SEM imaging of interface failure in globular splats reveals stress-concentration and splat sliding (a) and tortuous crack propagation (b) mechanisms during indentation. A bimodal distribution of critical stress for activating splat sliding in air-sprayed splats is shown in (c).

contrast to air-sprayed splats, the plastic flow was the prominent deformation mechanism here (Supplementary Videos V5 and V6). Fig. 5a shows the nucleation and propagation of shear bands across the splat due to indentation loading. Interestingly, despite the intense shearing, the interface resists cracking and splat detachment. The absence of cracking and the activation of plastic flow around the interface indicates metallurgical bonding between the splat and the substrate. Unlike the physical interlocking mechanism, metallurgical bonding requires the formation of chemical bonds. Therefore, pancake-shaped splats display superior resistance to detachment and displacement during indentation loading. The shear banding is accompanied by material pile-up due to tip penetration (Fig. 5b). It was shown in Fig. 1b that pancake-shaped splats are embedded inside the substrate due to high sonic velocity in lighter Helium gas. As a result, a significant portion of mechanical work during indentation is expended in gouging out the deposited micro-particle, resulting in pronounced pile-up (Supplementary Video V6). There were rare instances when microcracking was observed at the interface. Supplementary Video V7 demonstrates the crack formation was localized. Unlike globular splats, interfaces in pancake-shaped splats do not provide the path of least resistance for crack propagation. This is evident from Fig. 5c, where we see limited cracking without splat detachment and displacement.

These findings underscore the importance of intimate interfaces to prevent de-bonding and splat sliding. Post-spray heat-treatment has been reported to heal pores and micro-cracks in metallic coatings [24, 35]. To develop mechanistic insights into the effect of heat-treatment on interface bonding at the single splat length scale, we subjected the globular splats to the solution treatment-aging cycle described in Section 2.1. The heat-treated splats were characterized by intimate interfaces without micro-cracks or major pores (Fig. 6a) unlike as-sprayed specimens which displayed prominent signs of incomplete bonding (Fig. 3b). In-situ adhesion tests revealed some splats were displaced during tip penetration (Supplementary Video V8), while others resisted de-bonding and splat sliding (Supplementary Video V9). Mechanisms such as stress concentration followed by splat sliding, partial crack opening, and pure plastic deformation were observed at the splat/substrate interface (Fig. 6b, 6c, 6d). The plastic deformation mechanism, in particular, is in stark contrast to as-sprayed splats, which primarily demonstrated interfacial cracking followed by splat detachment. The prevalence of plastic deformation mechanism hints towards partial metallic bonding due to heat treatment. In the cases where the splat was displaced, the critical stress for splat sliding was calculated to be 4.1 MPa (± 600 kPa), which is over four times the average critical stress recorded for as-sprayed splats (Fig. 4c). These findings support the

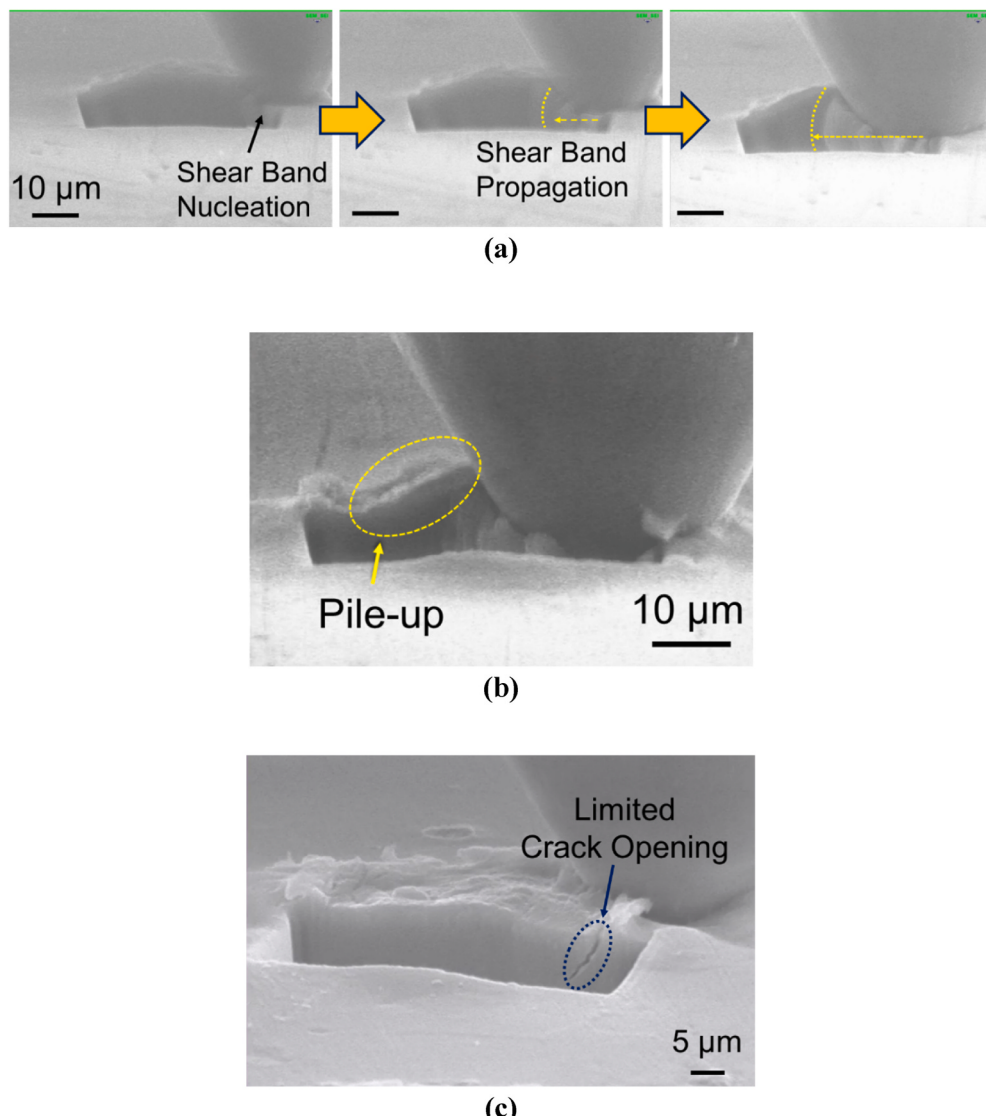


Fig. 5. Real-time SEM micrographs reveal the activation of shear band propagation (a), material pile-up (b), and limited crack opening (c) in pancake-shaped splats during in-situ indentation.

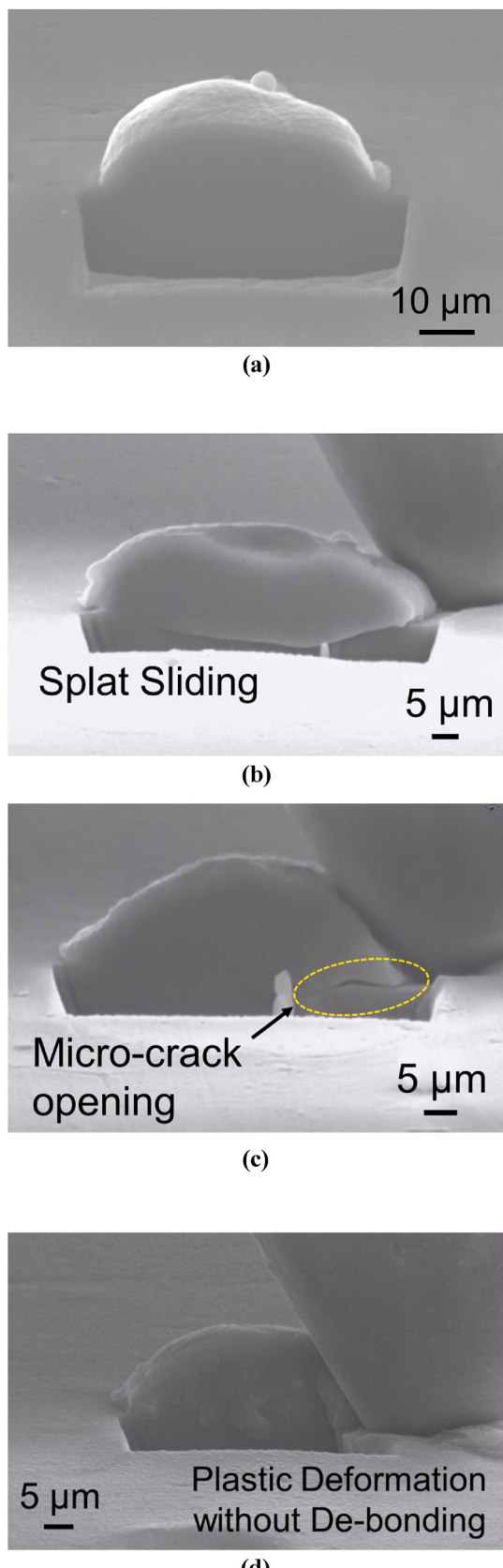


Fig. 6. In-situ SEM micrographs showing intimate splat-substrate bonding (a), splat sliding mechanism (b), localized crack opening (c), and pure plastic deformation (d) in heat-treated globular splats.

potency of heat-treatment for significantly improving interface bonding at the single splat length scale.

4. Discussion

The in-situ investigations in this work unravel a wide diversity of deformation mechanisms at splat/substrate interfaces. These mechanisms can be categorized into two broad classes, namely brittle failure and plastic response. Crack propagation, crack opening, and splat sliding fall under brittle failure; shear band propagation and material pile-up represent plastic deformation. Interestingly, when plasticity is dominant, the splat and the substrate deform as a single unit. Contrary to this, brittle failure involves detachment and displacement of the splat from its original position while the substrate exhibits plastic deformation. These differences in interface deformation modes suggest variation in the nature of bonding between the splat and the substrate. Metallic bonding and mechanical interlocking have been reported as the possible bonding mechanisms between cold sprayed coatings and substrates [48,49]. The metallic bonding is facilitated by clean metal-to-metal contact due to the fragmentation of the outer oxide shell on microparticles upon supersonic impact on the substrate [50]. On the other hand, the mechanical interlocking mechanism is attributed to the interfacial instabilities during deposition, resulting in interfacial waves, roll-ups, and vortices [48]. Additionally, the formation of lips on the substrate due to particle impact also leads to physical interlocking at the interface [9]. Since metallic bonding involves forming chemical bonds, the indentation-induced stresses should exceed the theoretical shear strength ($\sigma \geq \tau_{th}$) of Al to detach and displace the splat from the substrate. On the other hand, mechanical interlocking does not involve atom-level interactions, and therefore, splat de-bonding and sliding should be possible to activate at lower shear stresses ($\sigma < \tau_{th}$). The air-sprayed globular splats displayed a critical splat sliding stress ~ 1 MPa (Fig. 4c), which is 2 orders of magnitude lower than the theoretical shear strength of 6061Al (~ 207 MPa). This implies that globular splats do not form metallic bonds during supersonic impact. Pancake-shaped splats, on the other hand, resisted debonding within the instrument's load limit. Shear band propagation in the interface region indicates a preference for yielding over splat sliding. The tensile yield stress (σ_T) for the 6061 substrate is reported to be around 200 MPa [26]. The corresponding indentation yield stress (σ_I) can be determined using Tabor's relationship:

$$\frac{\sigma_I}{\sigma_T} = F \quad (2)$$

where F is a scaling factor. The most widely accepted value of F is around 3 [51]. Weaver and co-workers recently revisited the scaling factor's derivation for a conospherical tip by carefully performing micro-indentation experiments that considered early data points when the elastic-to-plastic transition occurs. The authors determined F 's value to be around 1.9 when a 6061Al alloy is indented using a conospherical probe [52]. Substituting the values of F and σ_T to Eq. (2) above, we obtain the indentation yield stress of 380 MPa for the pancake-shaped splat/substrate interface region. The local stresses near the interface should exceed the yield stress to initiate shear band propagation during indentation, seen in Fig. 5a. Since we did not notice splat sliding during shear band propagation, we can infer that the critical stress required to activate splat sliding in pancake-shaped splats exceeds the indentation yield stress. Therefore, we can conclude that metallic bonding is the key interface bonding mechanism in pancake-shaped splats.

The differences in the nature of bonding between globular (air-sprayed) and pancake-shaped (He-sprayed) splats can be understood by considering two mechanical effects during supersonic impact, namely, strain hardening and material softening. While the hardening behavior is due to the high strain rates involved during impact, material softening

occurs due to adiabatic heating at the splat/substrate interface [53]. The increase in interface temperature (T) is proportional to the plastic deformation (ϵ) of impacting particles, evident from the internal energy balance equation, $dT = \sigma d\epsilon / \rho c$, where σ is the flow stress, ρ is the mass density, and c is the specific heat [54]. Therefore, pronounced adiabatic interface heating is expected for He-sprayed splats due to significantly higher plastic strain (ϵ). The shear strength of microparticles falls to near-zero values due to thermal softening, which leads to the ejection of material jet upon impact [2]. The jetting event leads to the fragmentation of oxide shells on the outer surface of microparticles [55], enabling clean metal-to-metal contact for metallic bonding [19]. Recently, it has been argued that jetting can occur without thermal softening. A mechanism based on impact-induced shock has been proposed, stating that the release of pressure at the particle edge leads to jet formation [3]. Increasing the impact velocity results in a higher plastic strain at the interface and consequently pronounced localized tension that leads to jetting. Given the advantage of low-density Helium gas for achieving higher impact velocities, conditions are suitable for metallic bonding. A close look at the SEM micrograph in Fig. S3 confirms the formation of a ring of jet-like morphology around a He-sprayed particle. Contrary to this, air spray conditions adopted in this work are not sufficient to form strong metallic bonds. The key lesson learnt from these in-situ investigations is that the morphology evolution during supersonic impact is directly tied with the nature and strength of splat/substrate bonding. There is a transition from interlocking to metallurgical bonding as the plastic strain (ϵ) during particle impact increases.

We also demonstrated the efficacy of heat treatment in augmenting the adhesion and altering the deformation mechanisms at the single splat length scale. Heat-treatment has two independent effects on cold sprayed microstructures: (i) reduction of dislocation density within the splat [27] and (ii) solid-state diffusion between the splat and the substrate [17]. These phenomena should lead to enhanced ductility and interface failure resistance. In-situ measurements confirmed a jump in critical stress for splat sliding from under 1 MPa to over 4 MPa due to heat treatment. However, this value is significantly smaller than the theoretical shear strength of 6061Al (~207 MPa), indicating diffusion during heat treatment is not entirely successful in forming metallic bonds. It was mentioned before that impact and jetting lead to fragmentation and ejection of the oxide layer on Al particles. However, some of the oxide debris can accumulate and get trapped at the interface [15, 56]. Especially, relatively lower plastic strains when employing air as the carrier gas can suppress jetting, inhibiting oxide removal. These

oxide fragments hinder pure metal-to-metal contact and obstruct thermal diffusion between the splat and the substrate. As a result, complete metallurgical bonding does not take place despite prolonged heat treatment. Nevertheless, the observed four-fold enhancement in the critical stress value after the solution treatment and the aging cycle is promising. It underscores the suitability of heat treatment as a potent tool for solving bonding issues in cold sprayed deposits. A dedicated study on quantification of adhesion strength as a function of heat-treatment conditions will provide further insights into the diffusion time- and length scales desirable for stronger splat-substrate and splat-splat bonding.

The differences in adhesion and deformation behavior at the single splat length scale significantly impact bulk deposits' mechanical response. Fig. 7 compares the findings in this work (micro-scale deformation) with an earlier study on the flexural characterization of 6061Al coatings (macro-scale response) prepared using identical processing conditions [35]. The preferential activation of shear band propagation and pile-up in He-sprayed (pancake-shaped) splats translates to ductile behavior in the coating. Contrary to this, air-sprayed coatings demonstrate brittle-style failure, with catastrophic delamination of the coating from the substrate. This observation agrees with the interfacial crack propagation, splat detachment, and splat sliding mechanisms seen during in-situ adhesion measurements (Fig. 4). In the literature on cold sprayed alloys, cold sprayed materials' low ductility is often attributed to severe work hardening caused by powder particles' supersonic impact [7, 31]. However, the comparison of deformation behavior shown in Fig. 7 indicates otherwise. Even though He-sprayed splats and coatings experience higher plastic strains during deposition, they display superior ductility. This implies tailoring interface bonding is a more helpful strategy than tweaking the inherent plasticity of splats to control deposits' ductility. This assertion is supported by recently reported micromechanical investigations highlighting that impact velocity and post-spray heat-treatment do not affect the intrinsic flow stress of cold sprayed 6061Al splats [57]. The authors attributed this observation to dislocation saturation in Al splats, whereby the annihilation rate balances the dislocation multiplication rate due to dislocation cross-slip in FCC metals. The current work provides fundamental mechanistic insights into the role of processing and post-processing conditions in tuning the splat-substrate interfaces. Future studies will be devoted to understanding the mechanics of interfaces between two splats.

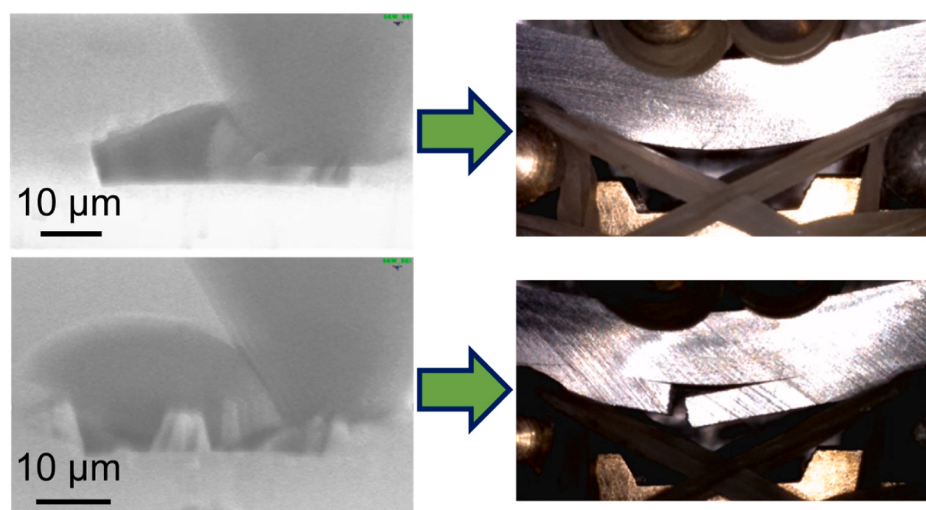


Fig. 7. A comparison of deformation mechanisms at the single splat scale with bulk deposits illustrates the importance of interface bonding to achieve superior ductility.

(The snapshots showing failure behavior of coatings are reproduced from the authors' earlier work [35])

5. Conclusion

We investigated the deformation and failure mechanisms associated with 6061Al splats deposited on 6061Al substrates. A novel in-situ test method is proposed, which harnesses the multi-axial stress field beneath an indenter probe to trigger interface de-bonding and splat sliding. The splats were sectioned by FIB milling to expose the buried interface, followed by in-situ indentation loading inside the SEM to capture the deformation mechanisms in real-time. Two sets of splat specimens with distinct morphologies were examined: (i) air-sprayed globular splats with limited flattening, and (ii) He-sprayed pancake-shaped splats with severe deformation. The effect of heat treatment on interface deformation was also evaluated. The key conclusions drawn from this work are:

- There is a transition from mechanical interlocking to metallurgical bonding at the splat/substrate interface with increasing particle flattening during cold spray deposition.
- Mechanically interlocked globular splats de-bond from the substrate via crack propagation and splat sliding mechanisms.
- Metallurgically bonded pancake splats resist debonding against indentation stresses exceeding 380 MPa, and the shear band propagation mechanism dominates the interface deformation.
- A two-step heat treatment, consisting of solution-treatment and aging, augmented the critical stress for splat sliding by a factor of 4.
- Plasticity-dominated deformation at interfaces translates to superior ductility in bulk deposits, underscoring the importance of interface engineering for preventing brittle failure seen in cold sprayed materials.

The in-situ approach described in this work provides a glimpse into the mechanics of interfaces at the single splat length scale for the first time. The current investigations were limited to splat/substrate interfaces. The future work will focus on understanding deformation and failure mechanisms at splat/splat interfaces created during coating build-up.

CRediT authorship contribution statement

Pranjal Nautiyal: Conceptualization, Methodology, Formal analysis. **Cheng Zhang:** Experimental process in coating deposition and characterization. **Benjamin Boesl:** Methodology. **Arvind Agarwal:** Conceptualization, Writing – review & editing, Supervision.

Declaration of competing interest

The authors declare that they have no known competing financial interests or personal relationships that could have appeared to influence the work reported in this paper.

Acknowledgments

This research was supported by the US Army Research Laboratory grants W911NF15-2-0026 (sub-award # 504108-78052) and W911NF2020256. The equipment support was provided by the Office of Naval Research through the DURIP grant (N00014-16-1-2604) and the National Science Foundation through the Engineering Research Centers program (NSF cooperative agreement # EEC-1647837). The authors thank the Arbegast Materials Processing & Joining Laboratory at South Dakota School of Mines & Technology for preparing samples investigated in this study. PN acknowledges Florida International University Graduate School for the Dissertation Year Fellowship award.

Appendix A. Supplementary data

Supplementary data to this article can be found online at <https://doi.org/10.1016/j.msea.2021.141828>.

Data availability

The raw/processed data required to reproduce these findings cannot be shared at this time as the data also forms part of an ongoing study.

References

- [1] F. Meng, D. Hu, Y. Gao, S. Yue, J. Song, Cold-spray bonding mechanisms and deposition efficiency prediction for particle/substrate with distinct deformability, Mater. Des. 109 (2016) 503–510, <https://doi.org/10.1016/j.matdes.2016.07.103>.
- [2] M. Hassani-gangaraj, D. Veysset, K.A. Nelson, C.A. Schuh, In-situ observations of single micro-particle impact bonding, Scr. Mater. 145 (2018) 9–13, <https://doi.org/10.1016/j.scriptamat.2017.09.042>.
- [3] M. Hassani-Gangaraj, D. Veysset, V.K. Champagne, K.A. Nelson, C.A. Schuh, Adiabatic shear instability is not necessary for adhesion in cold spray, Acta Mater. 158 (2018) 430–439, <https://doi.org/10.1016/j.actamat.2018.07.065>.
- [4] S. Suresh, S. Lee, M. Aindow, H.D. Brody, V.K. Champagne Jr., A.M. Dongare, Unraveling the mesoscale evolution of microstructure during supersonic impact of aluminum powder particles, Sci. Rep. 8 (2018) 10075, <https://doi.org/10.1038/s41598-018-28437-3>.
- [5] S. Suresh, S.W. Lee, M. Aindow, H.D. Brody, V.K. Champagne, A.M. Dongare, Mesoscale modeling of jet initiation behavior and microstructural evolution during cold spray single particle impact, Acta Mater. 182 (2020) 197–206, <https://doi.org/10.1016/j.actamat.2019.10.039>.
- [6] R.C. Dykhuizen, M.F. Smith, D.L. Gilmore, R.A. Neiser, X. Jiang, S. Sampath, Impact of high velocity cold spray particles, J. Therm. Spray Technol. 8 (1999) 559–564.
- [7] H. Assadi, H. Kreye, F. Gartner, T. Klassen, Cold spraying - a materials perspective, Acta Mater. 116 (2016) 382–407, <https://doi.org/10.1016/j.actamat.2016.06.034>.
- [8] P.C. King, S.H. Zahiri, M. Jahedi, Focused ion beam micro-dissection of cold-sprayed particles, Acta Mater. 56 (2008) 5617–5626, <https://doi.org/10.1016/j.actamat.2008.07.034>.
- [9] T. Hussain, D.G. Mccartney, P.H. Shipway, D. Zhang, Bonding mechanisms in cold Spraying : the contributions of metallurgical and mechanical components, J. Therm. Spray Technol. 18 (2009) 364–379, <https://doi.org/10.1007/s11666-009-9298-1>.
- [10] D. Goldbaum, R.R. Chromik, S. Yue, E. Irissou, J. Legoux, Mechanical property mapping of cold sprayed Ti splats and coatings, J. Therm. Spray Technol. 20 (2011) 486–496, <https://doi.org/10.1007/s11666-010-9546-4>.
- [11] M. Hassani-Gangaraj, D. Veysset, K.A. Nelson, C.A. Schuh, Melt-driven erosion in microparticle impact, Nat. Commun. 9 (2018) 5077, <https://doi.org/10.1038/s41467-018-07509-y>.
- [12] A.A. Tiamiyu, Y. Sun, K.A. Nelson, C.A. Schuh, Site-specific study of jetting, bonding, and local deformation during high-velocity metallic microparticle impact, Acta Mater. 202 (2021) 159–169, <https://doi.org/10.1016/j.actamat.2020.10.057>.
- [13] G. Bae, Y. Xiong, S. Kumar, K. Kang, C. Lee, General aspects of interface bonding in kinetic sprayed coatings, Acta Mater. 56 (2008) 4858–4868, <https://doi.org/10.1016/j.actamat.2008.06.003>.
- [14] M. Hassani, D. Veysset, Y. Sun, K.A. Nelson, C.A. Schuh, Microparticle impact-bonding modes for mismatched metals: from co-deformation to splattering and penetration, Acta Mater. 199 (2020) 480–494, <https://doi.org/10.1016/j.actamat.2020.08.038>.
- [15] K. Kang, S. Yoon, Y. Ji, C. Lee, Oxidation dependency of critical velocity for aluminum feedstock deposition in kinetic spraying process, Mater. Sci. Eng. A. 486 (2008) 300–307, <https://doi.org/10.1016/j.msea.2007.09.010>.
- [16] J. Lienhard, C. Crook, M.Z. Azar, M. Hassani, D.R. Mumm, D. Veysset, D. Apelian, K.A. Nelson, V. Champagne, A. Nardi, C.A. Schuh, L. Valdevit, Surface oxide and hydroxide effects on aluminum microparticle impact bonding, Acta Mater. 197 (2020) 28–39, <https://doi.org/10.1016/j.actamat.2020.07.011>.
- [17] C. Lee, J. Kim, Microstructure of kinetic spray coatings: a review, J. Therm. Spray Technol. 24 (2015) 592–610, <https://doi.org/10.1007/s11666-015-0223-5>.
- [18] D. Verma, J. Singh, A.H. Varma, V. Tomar, Evaluation of incoherent interface strength of solid-state-bonded Ti64/stainless steel under dynamic impact loading, JOM 67 (2015) 1694–1703, <https://doi.org/10.1007/s11837-015-1448-y>.
- [19] M. Hassani-Gangaraj, D. Veysset, K.A. Nelson, C.A. Schuh, Impact-bonding with aluminum, silver, and gold microparticles: toward understanding the role of native oxide layer, Appl. Surf. Sci. 476 (2019) 528–532, <https://doi.org/10.1016/j.apsusc.2019.01.111>.
- [20] M. Grujicic, C.L. Zhao, W.S. DeRosset, D. Helfritch, Adiabatic shear instability based mechanism for particles/substrate bonding in the cold-gas dynamic-spray process, Mater. Des. 25 (2004) 681–688, <https://doi.org/10.1016/j.matdes.2004.03.008>.
- [21] T. Schmidt, F. Gärtnner, H. Assadi, H. Kreye, Development of a generalized parameter window for cold spray deposition, Acta Mater. 54 (2006) 729–742, <https://doi.org/10.1016/j.actamat.2005.10.005>.
- [22] M.R. Rokni, A.T. Nardi, V.K. Champagne, S.R. Nutt, Effects of preprocessing on multi-direction properties of aluminum alloy cold-spray deposits, J. Therm. Spray Technol. 27 (2018) 818–826, <https://doi.org/10.1007/s11666-018-0723-1>.
- [23] Introduction to thermal spray processing, in: J.R. Davis (Ed.), Handb. Therm. Spray Technol., ASM International, Materials Park, 2004, pp. 3–13.
- [24] G. Sundararajan, N.M. Chavan, S. Kumar, The elastic modulus of cold spray coatings: influence of inter-splat boundary cracking, J. Therm. Spray Technol. 22 (2013) 1348–1357, <https://doi.org/10.1007/s11666-013-0034-5>.

- [25] B.A. Bedard, T.J. Flanagan, A.T. Ernst, A. Nardi, A.M. Dongare, H.D. Brody, V.K. Champagne, S.L.M. Aindow, Microstructure and micromechanical response in gas-atomized Al 6061 alloy powder and cold-sprayed splats, *J. Therm. Spray Technol.* 27 (2018) 1563–1578, <https://doi.org/10.1007/s11666-018-0785-0>.
- [26] M.R. Rokni, C.A. Widener, O.C. Ozdemir, G.A. Crawford, Microstructure and mechanical properties of cold sprayed 6061 Al in As-sprayed and heat treated condition, *Surf. Coat. Technol.* 309 (2017) 641–650, <https://doi.org/10.1016/j.surfcoat.2016.12.035>.
- [27] A.C. Hall, D.J. Cook, R.A. Neiser, T.J. Roemer, D.A. Hirschfeld, The effect of a simple annealing heat treatment on the mechanical properties of cold-sprayed aluminum, *J. Therm. Spray Technol.* 15 (2006) 233–238, <https://doi.org/10.1361/105996306X108138>.
- [28] W.B. Choi, L. Li, V. Luzin, R. Neiser, T. Gnäupel-Herold, H.J. Prask, S. Sampath, A. Gouldstone, Integrated characterization of cold sprayed aluminum coatings, *Acta Mater.* 55 (2007) 857–866, <https://doi.org/10.1016/j.actamat.2006.09.006>.
- [29] A.G. Gavras, D.A. Lados, V.K. Champagne, R.J. Warren, Effects of processing on microstructure evolution and fatigue crack growth mechanisms in cold-spray 6061 aluminum alloy, *Int. J. Fatigue.* 110 (2018) 49–62, <https://doi.org/10.1016/j.ijfatigue.2018.01.006>.
- [30] J.W. Murray, M.V. Zuccoli, T. Hussain, Heat treatment of cold-sprayed C355 Al for repair: microstructure and mechanical properties, *J. Therm. Spray Technol.* 27 (2018) 159–168, <https://doi.org/10.1007/s11666-017-0665-z>.
- [31] M.R. Rokni, C.A. Widener, V.K. Champagne, G.A. Crawford, S.R. Nutt, The effects of heat treatment on 7075 Al cold spray deposits, *Surf. Coat. Technol.* 310 (2017) 278–285, <https://doi.org/10.1016/j.surfcoat.2016.10.064>.
- [32] P. Vo, E. Iriessou, J.-G. Legoux, S. Yue, Mechanical and microstructural characterization of cold-sprayed Ti-6Al-4V after heat treatment, *J. Therm. Spray Technol.* 22 (2013) 954–964, <https://doi.org/10.1007/s11666-013-9945-4>.
- [33] M.R. Rokni, C.A. Widener, V.K. Champagne, G.A. Crawford, Microstructure and mechanical properties of cold sprayed 7075 deposition during non-isothermal annealing, *Surf. Coatings Technol.* 276 (2015) 305–315, <https://doi.org/10.1016/j.surfcoat.2015.07.016>.
- [34] R. Huang, M. Sone, W. Ma, H. Fukanuma, The effects of heat treatment on the mechanical properties of cold-sprayed coatings, *Surf. Coat. Technol.* 261 (2015) 278–288, <https://doi.org/10.1016/j.surfcoat.2014.11.017>.
- [35] P. Nautiyal, C. Zhang, V.K. Champagne, B. Boesl, A. Agarwal, In-situ mechanical investigation of the deformation of splat interfaces in cold-sprayed aluminum alloy, *Mater. Sci. Eng. A.* 737 (2018) 297–309, <https://doi.org/10.1016/j.msea.2018.09.065>.
- [36] Y. Chen, S.R. Bakshi, A. Agarwal, Intersplat friction force and splat sliding in a plasma-sprayed aluminum alloy coating during nanoindentation and microindentation, *ACS Appl. Mater. Interfaces* 1 (2009) 235–238, <https://doi.org/10.1021/am800114h>.
- [37] F. Tang, J.M. Schoenung, Evolution of Young's modulus of air plasma sprayed yttria-stabilized zirconia in thermally cycled thermal barrier coatings, *Scr. Mater.* 54 (2006) 1587–1592, <https://doi.org/10.1016/j.scriptamat.2006.01.021>.
- [38] P. Nautiyal, C. Zhang, V. Champagne, B. Boesl, A. Agarwal, In-situ creep deformation of cold-sprayed aluminum splats at elevated temperatures, *Surf. Coatings Technol.* 372 (2019) 353–360, <https://doi.org/10.1016/j.surfcoat.2019.05.045>.
- [39] A.G. Gavras, D.A. Lados, V.K. Champagne, R.J. Warren, D. Singh, Small fatigue crack growth mechanisms and interfacial stability in cold-spray 6061 aluminum alloys and coatings, *Metall. Mater. Trans. A.* 49 (2018) 6509–6520, <https://doi.org/10.1007/s11661-018-4929-0>.
- [40] D. Boruah, B. Robinson, T. London, H. Wu, H. De Villiers-Lovelock, P. Mcnutt, M. Doré, X. Zhang, Experimental evaluation of interfacial adhesion strength of cold sprayed Ti-6Al-4V thick coatings using an adhesive-free test method, *Surf. Coat. Technol.* 381 (2020) 125130, <https://doi.org/10.1016/j.surfcoat.2019.125130>.
- [41] D. Verma, M. Exner, V. Tomar, An investigation into strain rate dependent constitutive properties of a sandwiched epoxy interface, *Mater. Des.* 112 (2016) 345–356, <https://doi.org/10.1016/j.matdes.2016.09.068>.
- [42] ASM International Committee, *Heat Treating of Aluminum Alloys*, ASM International, 1991, <https://doi.org/10.1361/asmhb0001205>.
- [43] A.K. Keshri, D. Lahiri, A. Agarwal, Carbon nanotubes improve the adhesion strength of a ceramic splat to the steel substrate, *Carbon N. Y.* 49 (2011) 4340–4347, <https://doi.org/10.1016/j.carbon.2011.06.010>.
- [44] D. Lahiri, A. Agarwal, Scratch based technique quantifies adhesion strength at micro and nanoscales, *Adv. Mater. Process.* 170 (2012) 22–27, https://www.asminternational.org/en/news/magazines/-/journal_content/56/10192/A_MP17004P22/PERIODICAL-ARTICLE.
- [45] J.-H. Shin, S.-H. Kim, T.K. Ha, K.H. Oh, I.-S. Choi, H.N. Han, Nanoindentation study for deformation twinning of magnesium single crystal, *Scr. Mater.* 68 (2013) 483–486, <https://doi.org/10.1016/j.scriptamat.2012.11.030>.
- [46] R.C. Dykhuizen, M.F. Smith, Gas dynamic principles of cold spray gas, *J. Therm. Spray Technol.* 7 (1998) 205–212, <https://doi.org/10.1361/105996398770350945>.
- [47] I. Dowding, M. Hassani, Y. Sun, D. Veyset, K.A. Nelson, C.A. Schuh, Particle size effects in metallic microparticle impact-bonding, *Acta Mater.* 194 (2020) 40–48, <https://doi.org/10.1016/j.actamat.2020.04.044>.
- [48] M. Grujicic, J.R. Saylor, D.E. Beasley, W.S. Derosset, D. Helfritch, Computational analysis of the interfacial bonding between feed-powder particles and the substrate in the cold-gas dynamic-spray process, *Appl. Surf. Sci.* 219 (2003) 211–227, [https://doi.org/10.1016/S0169-4332\(03\)00643-3](https://doi.org/10.1016/S0169-4332(03)00643-3).
- [49] C. Chen, Y. Xie, R. Huang, S. Deng, Z. Ren, H. Liao, On the role of oxide film's cleaning effect into the metallurgical bonding during cold spray, *Mater. Lett.* 210 (2018) 199–202, <https://doi.org/10.1016/j.matlet.2017.09.024>.
- [50] C. Borchers, F. Gärtnert, T. Stoltenhoff, H. Kreye, Microstructural bonding features of cold sprayed face centered cubic metals, *J. Appl. Phys.* 96 (2004) 4288, <https://doi.org/10.1063/1.1789278>.
- [51] D. Tabor, *The Hardness of Metals*, Clarendon Press, Oxford, 1951.
- [52] J.S. Weaver, A. Khosravani, A. Castillo, S.R. Kalidindi, High throughput exploration of process-property linkages in Al-6061 using instrumented spherical microindentation and microstructurally graded samples, *Integr. Mater. Manuf. Innov.* 5 (2016) 192–211, <https://doi.org/10.1186/s40192-016-0054-3>.
- [53] H. Assadi, F. Gartner, T. Stoltenhoff, H. Kreye, Bonding mechanism in cold gas spraying, *Acta Mater.* 51 (2003) 4379–4394, [https://doi.org/10.1016/S1359-6454\(03\)00274-X](https://doi.org/10.1016/S1359-6454(03)00274-X).
- [54] G. Bae, S. Kumar, S. Yoon, K. Kang, H. Na, H.-J. Kim, C. Lee, Bonding features and associated mechanisms in kinetic sprayed titanium coatings, *Acta Mater.* 57 (2009) 5654–5666, <https://doi.org/10.1016/j.actamat.2009.07.061>.
- [55] W.-Y. Li, C.-J. Li, H. Liao, Significant influence of particle surface oxidation on deposition efficiency, interface microstructure and adhesive strength of cold-sprayed copper coatings, *Appl. Surf. Sci.* 256 (2010) 4953–4958, <https://doi.org/10.1016/j.apsusc.2010.03.008>.
- [56] K. Balani, A. Agarwal, S. Seal, J. Karthikeyan, Transmission electron microscopy of cold sprayed 1100 aluminum coating, *Scr. Mater.* 53 (2005) 845–850, <https://doi.org/10.1016/j.scriptamat.2005.06.008>.
- [57] T.J. Flanagan, B.A. Bedard, A.M. Dongare, H.D. Brody, A. Nardi, V.K. Champagne, M. Aindow, S.W. Lee, Mechanical properties of supersonic-impacted Al6061 powder particles, *Scripta Mater.* 171 (2019) 52–56, <https://doi.org/10.1016/j.scriptamat.2019.06.024>.